Assessing decadal changes in human exposure near wildfires in a Mediterranean region

scientific reports

OPEN

Assessing decadal changes in human exposure near wildfires in a Mediterranean region

Miguel Ángel Torres-Vázquez[1,2], Matteo Dalle Vaglie[3], Nicholas Kettridge[4], Federico Martellozzo[3], Gonzalo Miguez-Macho[5], Antonello Provenzale[6], Dominic Royé[7,8], Filippo Randelli[3] & Marco Turco[1]✉

This study examines the evolution of human exposure to wildfires in Catalonia, Spain, over the period 1992–2021, by integrating geospatial data on fire perimeters, population, satellite-derived nighttime light (NTL) imagery, and settlement records. Although the burned area shows a slight statistically non-significant decrease (-0.43 km^2/year), human exposure per unit of burned area has risen by 42% (based on GlobPOP data within burned areas) to 138% (based on GlobPOP data within a 5 km static buffer around fire perimeters), depending on the buffer distance and dataset used. This alarming trend is mainly driven by rapid urban expansion and population redistribution, particularly in coastal regions, which highlights a growing intersection between human settlements and fire-prone areas. Our findings emphasize the critical role of urbanization in amplifying wildfire risks, underscoring the urgent need to integrate demographic dynamics into fire risk governance strategies. By employing innovative proxies such as nighttime light data alongside high-resolution population and building density datasets, this study provides a comprehensive framework to assess wildfire exposure in rapidly urbanizing Mediterranean environments.

In Mediterranean coastal regions, urban expansion and climate change pose dual challenges[1,2]. Rising temperatures and prolonged droughts have increased the frequency, intensity, and duration of fire danger[1,3–5]. These trends are expected to persist and intensify due to the ongoing greenhouse gas emissions, further increasing the risk to human populations and infrastructure in vulnerable areas[6–8]. From a conceptual standpoint, we understand wildfire risk as the result of the interaction between three main components: hazard (the probability of wildfire occurrence), exposure (the presence of people and assets in fire-prone areas), and vulnerability (the susceptibility to damage). This formulation is commonly expressed through the equation: Risk = Hazard × Exposure × Vulnerability (see, e.g., reference[9]). Rapid urbanization in fire-prone regions amplifies wildfire impacts, raising significant concerns regarding public health, socio-economic stability, and environmental resilience[10–15]. The high frequency and intensity of wildfire events have resulted not only in widespread environmental and socio-economic damage but also in significant losses of life. Among Southern European countries (Spain, Portugal, France, Italy, and Greece), Spain ranks highest recorded forest fire-related deaths, with 346 from 1979 to 2016. These fatalities are predominantly clustered along the Mediterranean coast, particularly in regions like Catalonia and the Valencian Community, where rapid urban expansion into fire-prone areas has exacerbated wildfire risks[16]. This highlights the urgent need to better understand and mitigate human exposure to wildfires as urban development continues to expand on vulnerable landscapes.

Although strong evidence suggests that the Mediterranean biome is among the regions most affected by major wildfire disasters globally[17], with recent examples including events in the Iberian Peninsula (2017, 2025)[18,19], Greece (2023)[20], and Algeria (2021)[21], our understanding of the changing patterns of human exposure to fires in these regions remains limited[21].

[1]Regional Atmospheric Modelling (MAR) Group, Department of Physics, Regional Campus of International Excellence Campus Mare Nostrum (CEIR), University of Murcia, Murcia, Spain. [2]Environmental Remote Sensing Research Group, Department of Geology, Geography and the Environment, Universidad de Alcalá, Calle Colegios 2, 28801 Alcalá de Henares, Spain. [3]Dept. of Economics and Management, University of Florence, Florence, Italy. [4]School of Geography, Earth and Environmental Sciences, University of Birmingham, Birmingham B15 2TT, UK. [5]Non-Linear Physics Group, Faculty of Physics 15782, CRETUS, Universidade de Santiago de Compostela, Galicia, Spain. [6]Institute of Geosciences and Earth Resources (IGG), National Research Council (CNR), 56124 Pisa, Italy. [7]Biological Mission of Galicia (MBG), Spanish Council for Scientific Research (CSIC), Pontevedra, Spain. [8]Climate Research Foundation (FIC), Madrid, Spain. ✉email: marco.turco@um.es

Catalonia, a characteristic Mediterranean region and one of Europe's most fire-prone areas[16,22], provides an excellent case study for analysing human exposure to wildfires. Over recent decades, this region has experienced substantial urban development over recent decades, particularly in coastal areas, resulting in increased overlap between human settlements and fire-prone zones[1,16]. Despite advancements in forest management and fire suppression efforts, the socio-economic impacts of wildfires remain a growing concern as urbanized areas continue to expand into natural landscapes[22,23]. Moreover, Catalonia is one of the few regions in Europe that provides a publicly accessible long-term historical forest fire database, including detailed fire perimeters available since before the MODIS era[24,25], which is crucial for robust long-term assessments.

Understanding wildfire exposure also requires a resilience framework, which considers the adaptive capacity of communities to prepare for, respond to, and recover from fire events[26,27]. Catalonia's experience demonstrates the challenges of building resilience in rapidly urbanizing regions where fire risk is exacerbated by socio-economic pressures and climate change. By integrating resilience concepts, this study situates wildfire exposure within broader discussions of sustainable urban planning and disaster preparedness.

Moreover, the region exemplifies the dynamics of the wildland-urban interface (WUI), where expanding urban settlements intersect with natural landscapes prone to fire hazards[28,29]. The WUI is a critical zone of vulnerability, as it intensifies both the likelihood and consequences of wildfire events due to increased human activity and asset concentration[30]. As urban areas expand, particularly in coastal zones, this interface broadens, heightening the need for proactive risk management strategies[16]. Wildfire risk is especially pronounced in the Mediterranean basin, which accounts for 86% of the total burned area in the European Union[31]. Spain is among the most affected countries, with over 450,000 hectares burned annually in recent decades[31]. The WUI covers about 4.5% of Spain's territory, but in Catalonia, this figure exceeds 10%, reflecting a particularly high concentration of vulnerable areas[32–34].

This study leverages historical wildfire perimeter data, population records, settlement data, and satellite-derived nighttime light (NTL)[35] imagery to assess how human exposure to wildfires has evolved in Catalonia between 1992 and 2021. Here, NTL is used as a proxy for human activity and the intensity of built/urban infrastructure (electrification and settlement development). Because human exposure to wildfires is not fully captured by the resident population alone, we use heterogeneous proxies (NTL and building density) to represent complementary dimensions of exposure, evaluating them independently through their spatial overlay with wildfire perimeters. By incorporating innovative proxies such as NTL data[35–37], not previously used to measure fire exposure in this manner, alongside high-resolution demographic and building density datasets, this research offers a novel perspective on the interplay between urban growth and wildfire risk. To better understand the drivers of these trends, we also employ a counterfactual analysis, isolating the impact of population redistribution and urban expansion from changes in fire activity alone.

The findings presented here highlight a substantial increase in human exposure to wildfires per unit burned area over the study period, emphasizing urbanization's pivotal role in amplifying wildfire risks. These results align with global trends observed in other fire-prone regions, such as California and Greece, where the expansion of the wildland-urban interface has similarly heightened vulnerability to fire hazards[28,29,38].

By situating Catalonia as a representative case, our study underscores the importance of integrating demographic factors into fire risk governance strategies. It aims to contribute to broader discussions on sustainable urban planning and wildfire resilience in Mediterranean and other global contexts, offering actionable insights for policymakers and stakeholders.

Results

Figure 1 provides a multi-faceted view of key indicators: fire activity, human presence, and urbanization in Catalonia from 1992 to 2021. Figure 1a plots the total annual burned area (BA; ≥ 10 ha), revealing strong annual variability. Year 1994 stands out with a BA approaching 850 km^2, far exceeding the average (~ 70 km^2) and median (~ 16 km^2) for 1992–2021. Such an extreme year underscores the region's vulnerability. Beyond variability, the data suggest a negative trend in BA, with a − 0.43 km^2/year (not statistically significant). This contrasts with reference[22], who reported a significant decline in BA (− 7.3 km^2/year, $p < 0.05$) for 1983–2010. The discrepancy may stem from excluding the 1980s, a period of high fire activity. Figure 1b illustrates the spatial distribution of fire polygons, showing a strong concentration in coastal and pre-coastal areas, with large events (e.g., 1994) plainly visible.

In terms of human activity, Fig. 1c depicts changes in nighttime light intensity (NTL), serving as a proxy for human presence. We express trend estimates as a percentage 1992–2021 relative to the mean of the entire study period. Across Catalonia, NTL increased by 41% reflecting rapid urbanization and infrastructural growth (Supplementary Fig. 1a). Meanwhile, Fig. 1d shows population changes (GlobPOP), which vary widely; some areas show growth, especially the coastal urban zone, whereas others -often rural- experience declines. Over the study period, the population in Catalonia grew by ~ 78,600 people/year, leading to a 33% increase (Supplementary Fig. 1b). Notably, NTL and GlobPOP do not always correlate perfectly at the pixel level, reflecting different aspects of urban expansion (e.g., NTL can rise even where population is stable due to new infrastructure). In fact, the spatiotemporal correlation between NTL and GlobPOP shows positive and negative values (average absolute correlation of 0.5; Supplementary Fig. 2a).

Building density (HISDAC-ES) also grew substantially (Fig. 1e). Between 1995 and 2020, the number of buildings rose by ~ 21% overall, aligning with significant urban expansion. At the resolution matching NTL (~ 0.64 km), this increase is ~ 17% (Supplementary Fig. 3). Suburban and peri-urban zones experienced the largest gains, often closer to vegetation, hence more vulnerable to wildfires. This pattern is consistent with Fig. 1c, where NTL growth is notably high along urban fringes. A strong correlation emerges between NTL and HISDAC-ES, reaching an absolute average of 0.9 in areas where it is significant ($p < 0.05$; Supplementary Fig. 2b). Supplementary Fig. 2c shows the spatial correlation for each year between NTL and GlobPOP (blue line) and

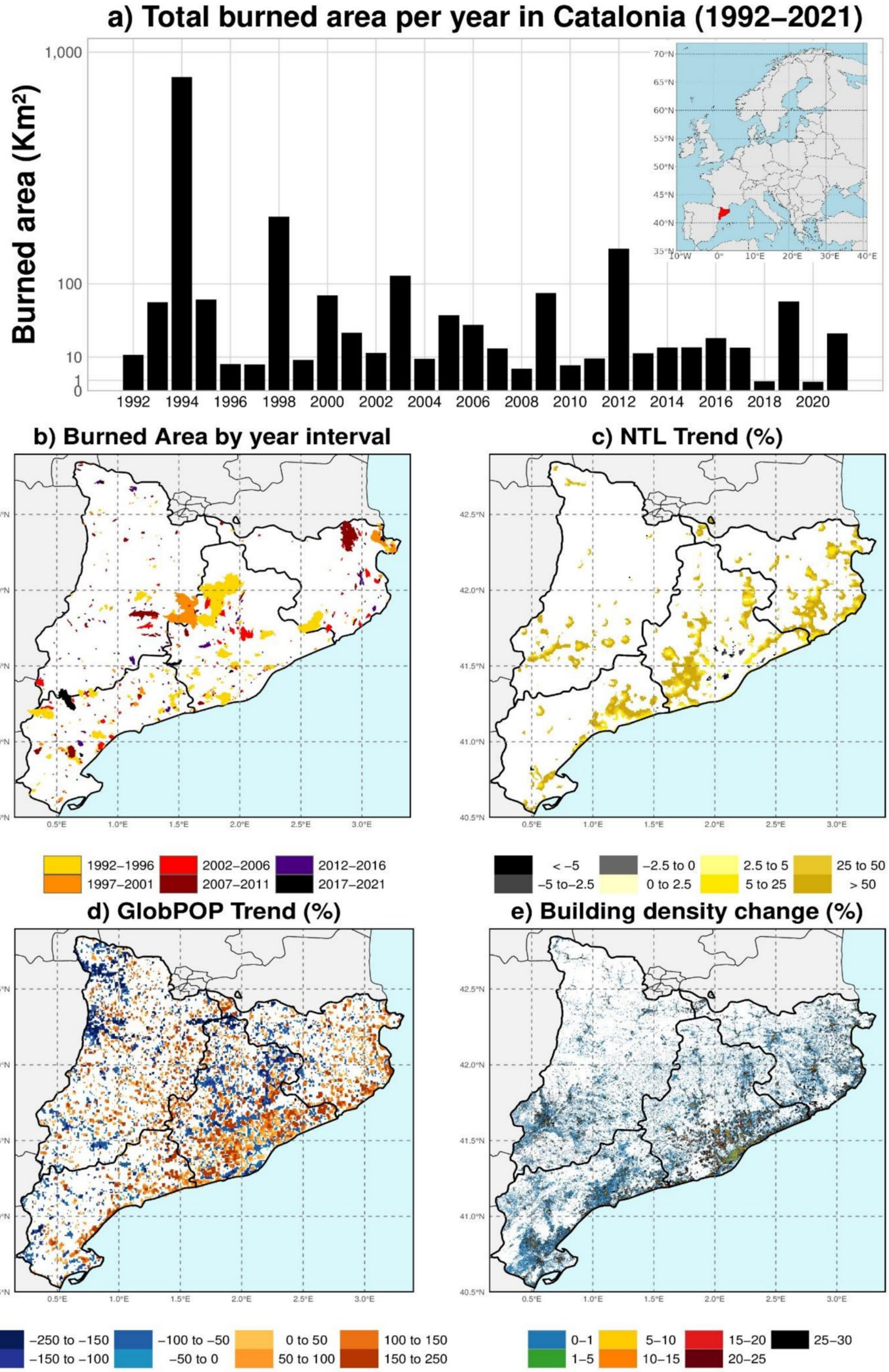

Fig. 1. Trends in burned area, nighttime lights, population, and building development in Catalonia (1992–2021). (**a**) Total annual burned area (km^2) in Catalonia and the location of Catalonia in Europe. (**b**) Spatial distribution of fire polygons by year. (**c**) Trend of nighttime light (NTL) data. (**d**) Population trend based on the GlobPOP. (**e**) Spatial percentage change in building density (HISDAC-ES) between 1995 and 2020. Trend units in (c) and (d) represent the total change as a percentage of the historical average for each period. Only significant trends ($p < 0.05$) are displayed.

between NTL and HISDAC-ES (red dots). The correlation between NTL and GlobPOP ranges from 0.66 to 0.82, while the correlation between NTL and HISDAC-ES remains around 0.53, both being statistically significant ($p < 0.05$).

Overall, these indicators underscore the importance of assessing how human exposure to wildfires has evolved, especially in the context of urbanization and development in fire-prone areas.

Figure 2 shows a marked increase in total population exposure (ET) per unit burned area (≥ 10 ha) from 1992 to 2021, regardless of the human proxies used (Fig. 2a, c, and e). For example, ET based on NTL increased by 63% (relative to its average) in directly burned areas and by 68% in a 5 km buffer. Likewise, GlobPOP-based exposure rose by 21% and 76%, respectively. To isolate the impact of population/human activity changes, we created a counterfactual scenario (ET^{92}) fixing the population/human proxies at 1992 (1995 for HISDAC-ES). The observed upward trends in ET—ET^{92} (Fig. 2b, d, and f) confirm that population redistribution and urban growth have significantly increased human exposure over the study period. For instance, NTL-based ET—ET^{92} rose by 175% in burned areas and 92% in a 5 km buffer, while GlobPOP-based ET—ET^{92} increased by 42% and 138%, respectively. Additionally, to assess the sensitivity of the results to fire selection, we compared normalized human exposure per burned area (ET/BA) between all wildfires ≥ 10 ha and the subset of large wildfires (≥ 100 ha), for a year with very high fire activity (1994). Supplementary Fig. 4 shows that both exposure proxies, nighttime lights (NTL) and population data (GlobPOP), present very strong linear relationships, with data points closely aligned along the 1:1 diagonal. This indicates high consistency between exposure estimates derived from all wildfires and those based solely on large wildfires. The alignment of the values corresponding to both dynamic buffers (10%, 50%, 90%) and static ones (e.g., 0.5 km, 1 km, 2.5 km, 5 km) suggests that, in 1994, the choice of fire size threshold or buffer type had a limited effect on the resulting exposure estimates.

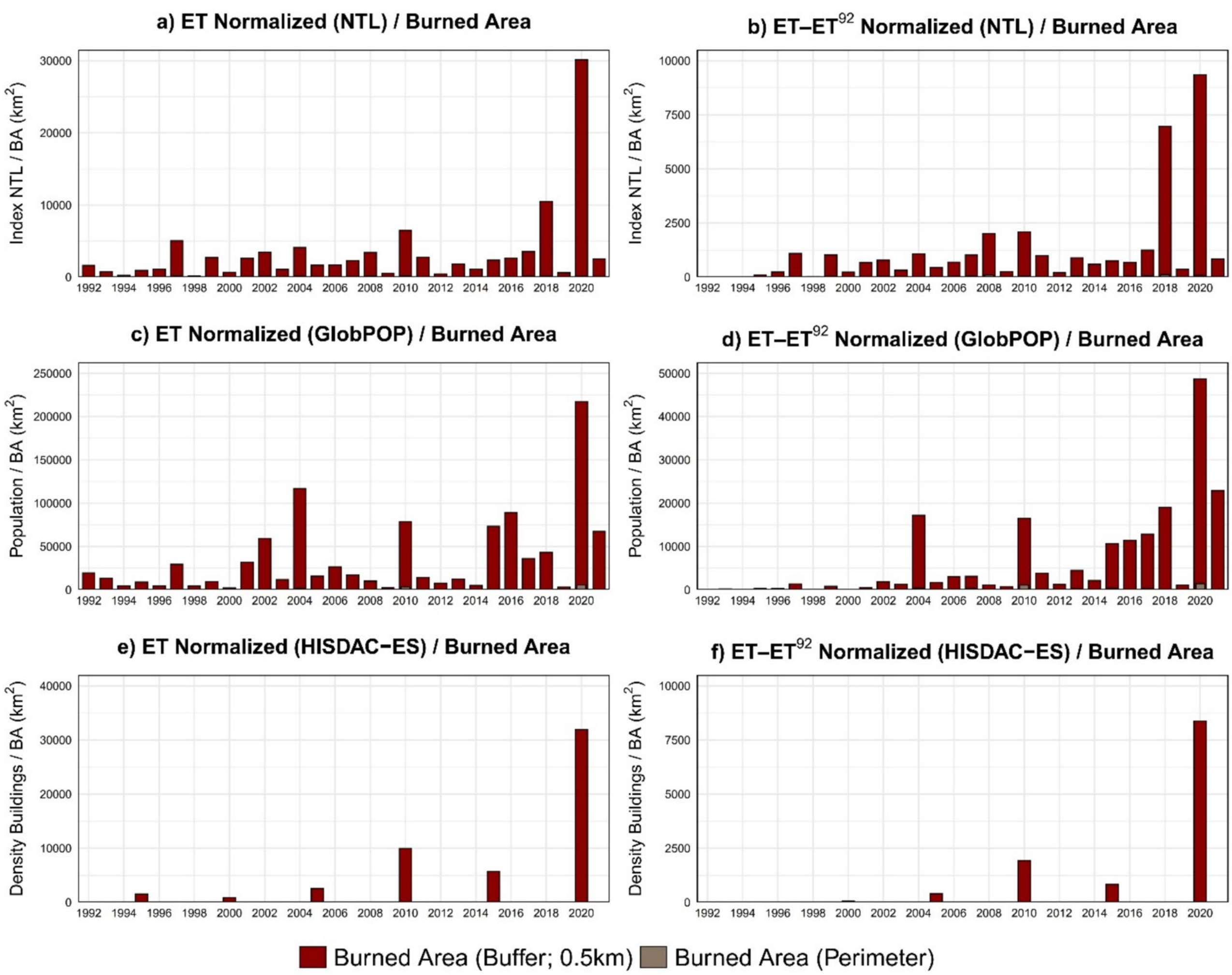

Fig. 2. Normalized human exposure to wildfires in Catalonia (1992–2021) using different datasets and counterfactual analysis for two buffer zones (0 km and 5 km). Panels (**a**), (**c**), and (**e**) show total exposure (ET) normalized by the burned area (BA), using NTL, GlobPOP, and HISDAC-ES, respectively. Panels (**b**), (**d**), and (**f**) illustrate ET- ET^{92}, the difference between total exposure in the actual scenario (ET) and the counterfactual ET^{92}, where population distribution is fixed at the 1992 (1995 for HISDAC-ES).

Although Figs. 2e and 2f (HISDAC-ES) lack annual resolution, they suggest similar patterns, indicating that increased building density also heightens wildfire exposure. To ensure comparability between indicators, we rescaled the HISDAC-ES data from its original resolution (100 m) to a coarser resolution (30 arcseconds, ~ 0.64 km in Catalonia), matching the spatial resolution of NTL and GlobPOP (see Supplementary Fig. 5). As expected, building density slightly decreases due to the smoothing effect inherent to spatial aggregation. However, the temporal trends and the relationship between urbanization and burned area remain consistent, which reinforces the robustness of the results.

Table 1 reports the correlation and trend analyses for the exposure metrics (ET and ET-ET^{92}) across dynamic buffers (scaled to each wildfire perimeter; r10%, r50%, r90%) in addition to the traditional static buffers of 0.5 km, 1 km, 2.5 km, and 5 km. The top section shows the correlation between NTL- and GlobPOP-based exposure (> 0.65, $p < 0.01$). Within the dynamic buffers, the agreement peaks in the r10% ring ($r = 0.67$), while in the static scheme, the highest value appears at 2.5 km ($r = 0.83$). In the middle section, positive trends in ET and (ET—ET^{92}) underscore the growing exposure driven by population growth and urban sprawl.

For the dynamic buffers, NTL (ET—ET^{92}) rises by up to 182% in r90%, and GlobPOP (ET—ET^{92}) by 167% in that same ring. In comparison, the static buffers show increases of 138% (NTL) and 268% (GlobPOP) in the 0.5 km zone. The last section of the table quantifies dynamic changes between the ET^{92} trend and the ET trend, expressed as a percentage. This metric reflects the extent to which recent exposure trends can be explained by processes that were already underway in 1992 (Supplementary Table 1 provides further details). This metric allows us to estimate the extent to which the observed increase in human exposure near wildfires can be attributed to processes already underway in 1992. In dynamic buffers (adjusted to the extent of each fire), NTL-based exposure shows negative values (e.g., -25% in r10 and -23% in r90), indicating that recent growth in nighttime light occurred in areas where there were no signs of exposure in 1992. In contrast, GlobPOP-based exposure in those same buffers remains positive (~ 40%), suggesting that recent population growth partially follows demographic dynamics already active in the early 1990s. In static buffers (the same for all fires regardless of size), the historical continuity signal intensifies with distance: for NTL, the ET^{92}/ET ratio increases from + 7% at 0.5 km to + 46% at 5 km, indicating that areas farther from the fire already had illuminated infrastructure in 1992. Meanwhile, GlobPOP remains around + 50% at all distances, reflecting a historically stable population distribution in the surrounding landscape. These results highlight the need for targeted mitigation where human activities intersect with fire-prone landscapes.

Discussion

These findings demonstrate a marked increase in human exposure to wildfires in Catalonia over the past three decades, largely fueled by rapid urbanization and population shifts in coastal and peri-urban areas. This trend is consistent with global patterns in wildfire-prone regions, such as California, Australia, and Greece, where WUI expansion has magnified the frequency and severity of wildfire events[14,15,17,28]. In California, for instance, the devastating 2018 Camp Fire underscored WUI vulnerabilities exacerbated by land-use policies favoring development in fire-prone zones[39], a concern further highlighted by the 2025 wildfires in Los Angeles. Similarly, Greece's recurrent fire disasters emphasize the persistent challenges in managing urban expansion in high-risk regions[20]. While these parallels affirm the global relevance of Catalonia's trajectory, the region also has distinctive socio-economic and ecological attributes. For example, NTL data provide an innovative measure of urbanization and economic activity, but they have limitations, including saturation effects in highly urbanized areas and the inability to capture temporary population fluctuations (e.g., tourism)[35,36]. Given that Catalonia hosts ~ 22 million tourists annually[40], these omissions could be significant, especially during peak wildfire seasons.

Methodologically, this study is readily transferable, but data limitations warrant caution. NTL harmonization efforts (DMSP-VIIRS) still contend with spatial resolution differences, saturation, and interannual

	Perimeter	Dynamic Buffers			Static Buffers			
ET Correlation	**Perimeter**	**r10%**	**r50%**	**r90%**	**0.5 km**	**1 km**	**2.5 km**	**5 km**
NTLvs.GlobPOP ET	0.65***	0.66***	0.73***	0.72***	0.78***	0.78***	0.83***	0.80***
Trend (%)	**Perimeter**	**ratio 10%**	**ratio 50%**	**ratio 90%**	**0.5 km**	**1 km**	**2.5 km**	**5 km**
NTL ET	63	55	51	41*	70*	74*	71***	69***
NTL ET-ET^{92}	175***	176***	171***	184***	139***	139***	110***	92***
GlobPOP ET	21	22	50	60	67	51*	64*	76*
GlobPOP ET-ET^{92}	42*	50**	94***	166***	273***	229***	174***	138***
Dynamic change (%)	**Perimeter**	**r10%**	**r50%**	**r90%**	**0.5 km**	**1 km**	**2.5 km**	**5 km**
NTL ET^{92}/ET	-19	-29	-27	-29	4	13	26	46
GlobPOP ET^{92}/ET	18	32	36	32	48	60	51	53

Table 1. Correlation, trend, and dynamic change analysis of exposure metrics normalized by burned area across different buffer distances. The analysis includes both static buffers (0.5 km, 1 km, 2.5 km, and 5 km) and dynamic buffers scaled to each wildfire perimeter (r10%, r50%, r90%). Trends are expressed as percent changes over the 30 years (1992–2021) relative to the mean for the entire period. Statistically significant values are noted by asterisks (* for $p < 0.1$, ** for $p < 0.05$, and *** for $p < 0.01$). Dynamic changes are the percent contribution of ET^{92} relative to ET.

inconsistencies[35]. GlobPOP offers integrated, continuous population estimates, yet any modeling or auxiliary-data bias can affect local accuracy[41]. Likewise, such datasets omit temporary population surges (e.g., tourism). HISDAC-ES building data, though high-resolution, relies on historical cadastral records that may vary in completeness[23]. Likewise, using polygons to represent burned area can miss unburned patches within fire boundaries and reflect changes in detection methods[42,43]. In certain rural areas, the presence of nighttime light does not always reflect continuous human activity or active landscape management. Some illuminated settlements, particularly those affected by demographic decline, may be surrounded by unmanaged vegetation, favoring fuel accumulation and increasing fire risk, as noted by reference[33]. Therefore, future analyses could benefit from integrating dynamic land use and fuel load indicators to improve exposure assessment in these transitional landscapes. Future enhancements should focus on mitigating these limitations and incorporating more granular data and dynamic variables (e.g., land use changes, fuel load indicators, tourism flows) to enhance exposure assessments in these transitional landscapes.

This study concentrates on direct human exposure (e.g., fire contact, smoke inhalation, extreme heat). However, indirect impacts, such as poor air quality, mental health effects, and long-term morbidity, extend beyond fire perimeters[20]. Rising exposure magnifies public health risks, including respiratory illnesses and psychological impacts[10,44]. Infrastructure disruptions further underscore the importance of integrated resilience planning. Consequently, policymakers must prioritize land-use controls and zoning measures that factor in wildfire risk. Community preparedness, early warning systems, and climate services are also essential components of adapting to an increasingly fire-prone future.

By highlighting how urbanization affects wildfire exposure, this work offers valuable insights for sustainable development and wildfire resilience. Despite data limitations, the framework presented here contributes to the broader goal of understanding human-wildfire interactions amid climate change.

This study provides a comprehensive assessment of three decades (1992–2021) of human exposure to wildfires in Catalonia, integrating long-term fire perimeter data, high-resolution population datasets, and Nighttime Light (NTL) data. Our results show a substantial rise in human exposure per unit burned area, primarily driven by the increasing overlap between urban infrastructure and fire-prone ecosystems.

By employing a counterfactual scenario fixing the 1992 population distribution, we quantified the contribution of demographic and land-use changes-accounting for up to 79% of the observed rise in exposure. This underscores how shifts in population patterns and urban development, particularly along coastal areas, underpin wildfire vulnerability. Additionally, the growing concentration of burned area in fewer large wildfires further exacerbates exposure[45]. Meanwhile, overall burned area displayed a non-significant decline, possibly reflecting improved forest management and fire suppression[46]. Yet, future climate scenarios project increases in fire danger, potentially reversing burned-area trends. Hence, focusing solely on burned-area metrics risks overlooking evolving exposure patterns[29]. In fact, identifying who and what is burning provides more actionable insights for anticipating future fire disasters.

To adapt, urban planning must integrate fire risk in zoning and building codes, while proactive strategies, such as fire hazard mapping, early warning systems, and community education[47], are critical at the wildland-urban interface. On the mitigation front, rapid greenhouse gas emission reductions are paramount to limit increases in fire danger. By combining adaptation and mitigation, societies can pursue a more resilient coexistence with fire, minimizing adverse impacts while recognizing fire's ecological roles[44].

Data and methods

We used the Harmonized Global Nighttime Lights Dataset version 8, spanning 1992 to 2021 with a spatial resolution of 30 arc seconds (~0.64 km in Catalonia), as presented by references[44,48]. This dataset integrates observations from the Defense Meteorological Satellite Program (DMSP) and the Visible Infrared Imaging Radiometer Suite (VIIRS), providing a consistent time series of nighttime light data expressed as harmonised digital numbers (DN) ranging from 0 to 63. These DN values are adimensional indices that represent the relative intensity of artificial nighttime lighting in each pixel and are commonly used as a proxy for human presence and activity. However, there are uncertainties in NTL pixels with values less than or equal to 10, so we excluded these low values from our analysis, as recommended by reference[35].

Additionally, we utilized the Global Gridded Population Dataset (GlobPOP Version 2.0) by references[41,49] for the common period 1992–2021. The GlobPOP dataset offers key advantages: it provides consistent annual population estimates at a high spatial resolution of 30 arc seconds, even for years before 2000 -an improvement over standard global population datasets that typically offer only five-year intervals and lack coverage before 2000. The annual total population from GlobPOP was compared with the official estimates from the Statistical Institute of Catalonia (Idescat S2)[40], showing a very high correlation (0.98, $p < 0.05$) and a bias of 4.2%, indicating strong agreement between both sources (see Supplementary Fig. 1).

We also used the dataset HISDAC-ES version 2 of the historical settlement dataset for Spain, as described by reference[50]. This comprehensive compilation draws from cadastral data spanning 1900–2020, providing gridded surfaces at 100 m resolution every five years. Such detailed spatiotemporal information on settlement and urbanization patterns is critical for understanding various natural, anthropogenic, and social processes. In our analysis, we focused on the *Building Density* variable, which measures the number of buildings in a defined area. To make it comparable with NTL and GlobPOP (30 arc-seconds), the Building Density layer was aggregated from 100 m to 30 arc-seconds by summing the 100 m cells contained within each 30 arc-second cell.

Finally, we used annual fire-perimeter polygons from 1992 to 2021, obtained through the reference[24]. This period was selected to match the availability of NTL data. The fire perimeter dataset is regularly updated and revised, with fire polygons derived from official forest fire reports, GPS-based mappings by rural agents, remote sensing imagery (e.g., Landsat and Sentinel-2), and airborne sensors. The version used in this study was last updated on May 3, 2024. Although this dataset cannot be considered as an absolute ground truth, it is widely

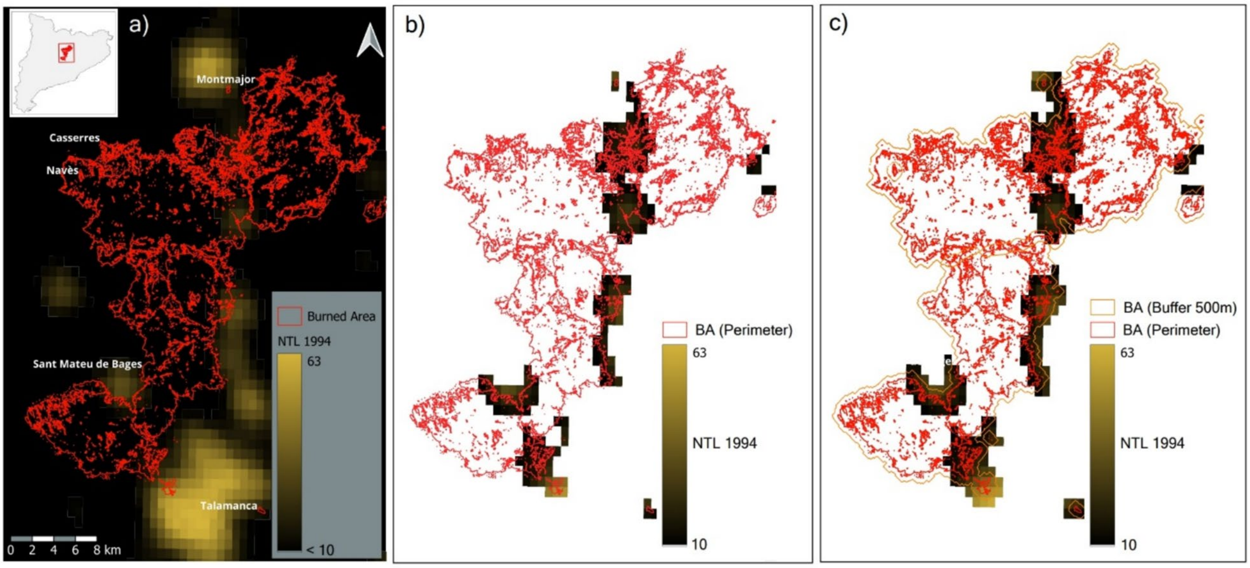

Fig. 3. Example of burned area perimeters and nighttime lights (NTL) in 1994. (**a**) Full scene with NTL beneath the Burned Area (BA; 1994) perimeters. The polygons are shown as red outlines. NTL is represented using harmonised digital numbers (DN; 0–63). The inset indicates the location within Catalonia. The names shown within panel (a) correspond to the municipalities covered by the fire-perimeter polygons. (**b**) NTL values (DN ≥ 10) retained only where they intersect the BA perimeter (red). (**c**) NTL values (DN ≥ 10) retained within a 500 m buffer around the BA perimeters (buffer outline in orange; BA perimeter in red).

regarded as the best available source of official fire statistics and has been used extensively (see e.g., reference[51]). For additional details, we refer to reference[24]. To maintain data homogeneity, we only analysed fires with a surface area ≥ 10 ha were considered. As shown in Supplementary Fig. 6, for much of the study period, fires below this threshold were not consistently recorded, ensuring consistency.

To estimate human exposure to fire, we extracted the human activity data (NTL, GlobPOP, or Building Density [HISDAC-ES]) intersecting with the fire perimeters and summed the exposed intersection for each year across the entire region of Catalonia. This was done using the mask function from the terra R package, which retains raster values only within the specified vector geometry. Proxy agreement was quantified using Spearman correlations after harmonisation in three complementary ways: (i) pixel-wise temporal correlations between annual NTL and GlobPOP time series (1992–2021) and between NTL and HISDAC-ES over overlapping years (1995–2020) to map spatiotemporal agreement (Supplementary Fig. 2a-b); (ii) year-wise spatial correlations across pixels within Catalonia (Supplementary Fig. 2c); and (iii) correlations between the annual exposure series derived from NTL and GlobPOP for each buffer definition (Table 1).

To assess the influence of fire size on surrounding exposure, we first conducted an analysis using dynamic buffers, with radii defined individually for each fire event. Specifically, we applied three dynamic thresholds (r10, r50, and r90), corresponding to the radius of a circle with an area equal to the 10th, 50th, and 90th percentiles of the burned area distribution. These dynamic buffers were calculated as:

$$r_i = \sqrt{\frac{A_i}{\pi}}$$

where A_i is the burned area of the fire i, in km^2. This approach ensures that smaller fires are surrounded by proportionally smaller buffers, while larger fires are assigned broader zones of influence, in line with their actual magnitude. As a complementary analysis, we also applied static buffers around fire perimeters, following the fixed-distance buffer scheme used in reference[38] to characterise near-fire exposure (0.5 km, 1 km, 2.5 km, and 5 km). Exposure was calculated independently for each year and buffer distance, so that overlapping buffer areas did not result in duplicated values. Annual exposure estimates, therefore, reflect non-redundant population or activity within the spatial extent of fire events for each year. To facilitate interpretation, Fig. 3 shows this workflow for a representative year (1994; the worst year in the historical series; see also the Results section), showing the NTL pixels retained within the fire perimeter (Fig. 3b) and within a 0.5-km buffer (Fig. 3c).

To evaluate temporal changes, we calculated the slopes of the time series using the Theil-Sen estimator and evaluated significance with the modified Mann–Kendall test for serially correlated data, applying the variance correction proposed by reference[52]. Implementation was done with the *mmkh* function in the modifiedmk package in R. Spearman's rank correlation was used to assess relationships among data, with significance determined via Student's t-distribution.

Data availability

The datasets used in this study are publicly available. Nighttime light data, harmonized from DMSP and VIIRS for 1992-2021, can be accessed through figshare at https://doi.org/10.6084/m9.figshare.9828827.v8. The GlobPOP dataset, offering global gridded population data for 1990-2022, is available on Zenodo at https://doi.org/10.5281/zenodo.11179644. The HISDAC-ES dataset (historical settlement data for Spain, 1900 to 2020) is accessible via https://doi.org/10.6084/m9.figshare.22009643.v2. Fire perimeter data for Catalonia is found at https://agricultura.gencat.cat/ca/serveis/cartografia-sig/bases-cartografiques/boscos/incendis-forestals/incendis-forestals-format-shp/. The region of Catalonia was obtained using the R library *rnaturalearth*. The analysis code is available upon request from the corresponding author.

Received: 12 February 2025; Accepted: 6 January 2026
Published online: 20 January 2026

References

1. González-Leonardo, M., Newsham, N. & Rowe, F. Understanding population decline trajectories in Spain using sequence analysis. *Geogr. Anal.* **55**, 495–516 (2023).
2. IPCC. Climate Change 2021: The Physical Science Basis. *Contribution of Working Group I to the Sixth Assessment Report of the Intergovernmental Panel on Climate Change*. (eds Masson-Delmotte, V. et al) Cambridge Univ. Press. https://doi.org/10.1017/9781009157896 (2021).
3. Richardson, D. et al. Global increase in wildfire potential from compound fire weather and drought. *npj Clim. Atmos. Sci.* **5**, 23 (2022).
4. Jain, P., Castellanos-Acuna, D., Coogan, S. C., Abatzoglou, J. T. & Flannigan, M. D. Observed increases in extreme fire weather driven by atmospheric humidity and temperature. *Nat. Clim. Change.* **12**, 63–70 (2022).
5. El Garroussi, S., Di Giuseppe, F., Barnard, C. & Wetterhall, F. Europe faces up to tenfold increase in extreme fires in a warming climate. *npj Clim. Atmos. Sci.* **7**(1), 30 (2024).
6. Jones, M. W. et al. Global and regional trends and drivers of fire under climate change. *Rev. Geophys.* **60**, e2020RG000726 (2022).
7. Quilcaille, Y., Batibeniz, F., Ribeiro, A. F., Padrón, R. S. & Seneviratne, S. I. Fire weather index data under historical and shared socioeconomic pathway projections in the 6th phase of the Coupled Model Intercomparison Project from 1850 to 2100. *Earth Syst. Sci. Data.* **15**, 2153–2177 (2023).
8. Torres-Vázquez, M. Á. et al. Large increase In extreme fire weather synchronicity over Europe. *Environ. Res. Lett.* https://doi.org/10.1088/1748-9326/ada8c2 (2025).
9. San-Miguel-Ayanz, J., Moreno, J. M. & Camia, A. Analysis of large fires in European Mediterranean landscapes: Lessons learned and perspectives. *For. Ecol. Manag.* **294**, 11–22 (2013).
10. Chen, G. et al. Mortality risk attributable to wildfire-related PM2.5 pollution: A global time series study in 749 locations. *Lancet Planet. Health* **5**, e579–e587 (2021).
11. Ganteaume, A., Barbero, R., Jappiot, M. & Maillé, E. Understanding future changes to fires in southern Europe and their impacts on the wildland-urban interface. *JSSR* **2**, 20–29 (2021).
12. Chen, B. et al. Wildfire risk for global wildland-urban interface areas. *Nat. Sustain.* **7**, 474–484 (2024).
13. Chen, G. et al. All-cause, cardiovascular, and respiratory mortality and wildfire-related ozone: A multicountry two-stage time series analysis. *Lancet Planet. Health* **8**, e452–e462 (2024).
14. Tang, W., He, C., Emmons, L. & Zhang, J. Global expansion of wildland-urban interface (WUI) and WUI fires: Insights from a multiyear worldwide unified database (WUWUI). *Environ. Res. Lett.* **19**, 044028 (2024).
15. Guo, Y., Wang, J., Ge, Y. & Zhou, C. Global expansion of wildland-urban interface intensifies human exposure to wildfire risk in the 21st century. *Sci. Adv.* **10**, eado9587 (2024).
16. Molina-Terrén, D. M. et al. Analysis of forest fire fatalities in southern Europe: Spain, Portugal, Greece and Sardinia (Italy). *Int. J. Wildland Fire* **28**, 85–98 (2019).
17. Cunningham, C. X. et al. Climate-linked escalation of societally disastrous wildfires. *EcoEvoRxiv* https://doi.org/10.32942/X22622 (2024).
18. Turco, M. et al. Climate drivers of the 2017 devastating fires in Portugal. *Sci. Rep.* **9**, 13886 (2019).
19. Sánchez-Hernández, G. et al. Record-Breaking 2025 European Wildfires Concentrated in Northwest Iberia. *Glob. Change Biol.* **31**, e70649 (2025).
20. Jones, M. W. et al. State of wildfires 2023–2024. *Earth Syst. Sci. Data.* **16**, 3601–3685 (2024).
21. San-Miguel-Ayanz, J. et al. Forest Fires in Europe, Middle East and North Africa 2021. Publications Office of the European Union. https://doi.org/10.2760/34094 (2022).
22. Turco, M., Llasat, M. C., Tudela, A., Castro, X. & Provenzale, A. Brief communication Decreasing fires in a Mediterranean region (1970–2010, NE Spain). *NHESS* **13**, 649–652 (2013).
23. Uhl, J. H. et al. HISDAC-ES: Historical settlement data compilation for Spain (1900–2020). *Earth Syst. Sci. Data.* **15**, 4713–4747 (2023).
24. Generalitat de Catalunya. Forest fire cartographic database. Retrieved from https://agricultura.gencat.cat/ca/serveis/cartografia-sig/bases-cartografiques/boscos/incendis-forestals/incendis-forestals-format-shp/ (2024).
25. Gincheva, A. et al. A monthly gridded burned area database of national wildland fire data. *Sci. Data* **11**, 352 (2024).
26. Walker, B., Holling, C. S., Carpenter, S. R. & Kinzig, A. Resilience, adaptability and transformability in social-ecological systems. *Ecol. Soc.* **9**, 12 (2004).
27. Moritz, M. et al. Learning to coexist with wildfire. *Nature* **515**, 58–66 (2014).
28. Bowman, D. M. Human exposure and sensitivity to globally extreme wildfire events. *Nat. Ecol. Evol.* **1**, 0058 (2017).
29. Kolden, C. Wildfires: Count lives and homes, not hectares burnt. *Nature* **586**, 9 (2020).
30. Radeloff, V. C. et al. The wildland-urban interface in the United States. *Ecol. Res.* **15**, 799–805 (2005).
31. Bar-Massada, A., Alcasena, F., Schug, F. & Radeloff, V. C. The wildland-urban interface in Europe: Spatial patterns and associations with socioeconomic and demographic variables. *Landsc. Urban Plann.* **235**, 104759 (2023).
32. Alcasena, F. J., Evers, C. R. & Vega-Garcia, C. The wildland-urban interface raster dataset of Catalonia. *Data Brief* **17**, 124–128 (2018).
33. Badia, A., Pallares-Barbera, M., Valldeperas, N. & Gisbert, M. Wildfires in the wildland-urban interface in Catalonia: Vulnerability analysis based on land use and land cover change. *Sci. Total Environ.* **673**, 184–196 (2019).
34. Beltrán-Marcos, D., Calvo, L., Fernández-Guisuraga, J. M., Fernández-García, V. & Suárez-Seoane, S. Wildland-urban interface typologies prone to high severity fires in Spain. *Sci. Total Environ.* **894**, 165000 (2023).
35. Li, X., Zhou, Y., Zhao, M. & Zhao, X. A harmonized global nighttime light dataset 1992–2018. *Sci. Data* **7**, 168 (2020).
36. Levin, N. et al. Remote sensing of night lights: A review and an outlook for the future. *Remote Sens. Environ.* **237**, 111443 (2020).
37. Ceola, S., Laio, F. & Montanari, A. Satellite nighttime lights reveal increasing human exposure to floods worldwide. *Geophys. Res. Lett.* **41**, 7184–7190 (2014).

38. Modaresi Rad, A. et al. Human and infrastructure exposure to large wildfires in the United States. *Nat. Sustain.* **6**, 1343–1413 (2023).
39. Troy, A. et al. An analysis of factors influencing structure loss resulting from the 2018 Camp Fire. *Int. J. Wildland Fire.* **31**, 586–598 (2022).
40. Institut d'Estadística de Catalunya (Idescat). (n.d.). *Tourism*. https://www.idescat.cat/tema/turis (2024).
41. Liu, L., Cao, X., Li, S. & Jie, N. A 31-year (1990–2020) global gridded population dataset generated by cluster analysis and statistical learning. *Sci. Data.* **11**, 124 (2024).
42. Leonard, S. W., Bennett, A. F. & Clarke, M. F. Determinants of the occurrence of unburnt forest patches: Potential biotic refuges within a large, intense wildfire in south-eastern Australia. *For. Ecol. Manag.* **314**, 85–93 (2014).
43. Turco, M. et al. Decreasing fires in Mediterranean Europe. *PLoS ONE* **11**, e0150663 (2016).
44. Johnston, F. et al. Interdisciplinary solutions and collaborations for wildfire management. *Iscience* **27**, 1–7 (2024).
45. Royé, D. et al. Wildfire burnt area patterns and trends in Western Mediterranean Europe via the application of a concentration index. *Land Degrad. Dev.* **31**, 311–324 (2020).
46. Turco, M., Llasat, M. C., von Hardenberg, J. & Provenzale, A. Climate change impacts on wildfires in a Mediterranean environment. *Clim. Change.* **125**, 369–380 (2014).
47. Trucchia, A. et al. Wildfire hazard mapping in the eastern Mediterranean landscape. *Int. J. Wildland Fire.* **32**, 417–434 (2023).
48. Li, X., Zhou, Y., Zhao, M. & Zhao, X. Harmonization of DMSP and VIIRS nighttime light data from 1992–2021 at the global scale. Sets. Figshare https://doi.org/10.6084/m9.figshare.9828827.v8 (2020).
49. Liu, L., Cao, X., Li, S. & Jie, N. GlobPOP: A 33-year (1990–2022) global gridded population dataset generated by cluster analysis and statistical learning (Version 2.0). Zenodo https://doi.org/10.5281/zenodo.11179644 (2024).
50. Uhl, J. H. et al. HISDAC-ES: Historical settlement data compilation for Spain (1900–2020). Sets. Figshare https://doi.org/10.6084/m9.figshare.22009643.v2 (2023).
51. González, J. R. & Pukkala, T. Characterization of forest fires in Catalonia (north-east Spain). *Eur. J. For. Res.* **126**, 421–429 (2007).
52. Hamed, K. H. & Rao, A. R. A modified Mann-Kendall trend test for autocorrelated data. *J. Hydrol.* **204**, 182–196 (1998).

Acknowledgements
This work was supported by the project 'Climate and Wildfire Interface Study for Europe (CHASE)' under the 6th Seed Funding Call by the European University for Well-Being (EUniWell). MAT-V has received funding from the European Space Agency (ESA) through the FireCCI project (contract No. 4000126706/19/I-NB), which enabled the publication costs of this article to be covered. MT acknowledges funding by the Spanish Ministry of Science, Innovation and Universities through the Ramón y Cajal Grant Reference RYC2019-027115-I and through the project ONFIRE, Grant PID2021-123193OB-I00, funded by MCIN/AEI/https://doi.org/10.13039/501100011033and by "ERDF A way of making Europe". AP acknowledges the support of the EU H2020 project "FirEUrisk", Grant Agreement No. 101003890. GMM acknowledges funding by the Spanish Ministry of Science, Innovation and Universities through project RIESPIRO (PID2021128510OB-I00). The authors thank the Generalitat de Catalunya for access to fire perimeter data and Xavier Castro from the Forest Fire Prevention Service of the Generalitat de Catalunya for the helpful discussions on the matter.

Author contributions
M.A.T.-V. designed the study, collected and processed the data, performed the analysis, and wrote the manuscript. M.T. contributed to the study design, analysis, manuscript writing, and secured funding. N.K., M.D.V., F.M., G.M.-M., A.P., D.R., and F.R. contributed substantially to the interpretation of the results, manuscript revisions, and scientific discussion.

Declaration

Competing interests
The authors declare no competing interests.

Additional information
Supplementary Information The online version contains supplementary material available at https://doi.org/10.1038/s41598-026-35426-4.

Correspondence and requests for materials should be addressed to M.T.

Reprints and permissions information is available at www.nature.com/reprints.

Publisher's note Springer Nature remains neutral with regard to jurisdictional claims in published maps and institutional affiliations.